Computational Modelling of Concrete Structures – Meschke, de Borst, Mang & Bićanić (eds)
 ISBN 0 415 39749 9

Lattice-cell approach to quasibrittle fracture modeling

Peter Grassl
University of Glasgow, Glasgow, UK

Zdeněk Bažant
Northwestern University, Evanston, IL, USA

Gianluca Cusatis
Rensselaer Polytechnic Institute, Troy, NY, USA

ABSTRACT: The present paper deals with a lattice-cell approach to fracture modeling. The struts in the lattice form triangular cells, which resist volume change and thus introduce a coupling of the constitutive responses of the struts. With this approach, the full range of Poisson's ratio of an elastic solid can be modeled. Poisson's ratio is controlled by the ratio of the material stiffness of the struts and the cells. The relationship of the parameters of the lattice-cell model to the parameters of the Hooke's law of the elastic solid in plane strain is derived using as an example an equilateral triangle. The validity of these derivations is supported by numerical simulation of an elastic solid in uniaxial tension. Furthermore, the constitutive response of the strut is extended to take into account the evolution of damage, which allows the simulation of fracture. The fracture process of a solid in plane strain subjected to uniaxial tension is studied. Both the positions of the vertices and the material strengths of the struts are assumed to be random. The results show that the lattice-cell model is able to describe the full range of Poisson's ratio of an elastic solid and still remains suitable for modeling fracture. So far, the model is limited to plane strain and tensile fracture.

1 INTRODUCTION

Lattice and particle models are known to be suitable for modeling fracture of materials such as concrete, rock, ceramics and ice (Bažant et al. (1990), Schlangen and van Mier (1992), Jirásek and Bažant (1995a), Jirásek and Bažant (1995b)). However, for lattice models composed of struts or particle models transmitting axial forces only it is known that Poisson's ratio of an elastic solid approaches, in the limit of an infinite number of elements (particles), the value of 1/4. This restriction can be overcome by introducing shear stiffnesses, either by replacing the struts by beams or, in the case of particle systems, by adding shear springs between particles. This approach was applied by Zubelewicz and Bažant (1987) and Morikawa et al. (1993) and investigated in greater detail by Griffiths and Mustoe (2001). The addition of shear stiffness allows it to model Poisson's ratios less than 1/4. Furthermore, the addition of shear springs in particle models allows it to simulate realistically the compressive failure of cohesive-frictional materials such as concrete, as it was shown by Cusatis et al. (2003a) and Cusatis et al. (2003b). Nevertheless, Poisson's ratios greater than 1/4 cannot be modeled by the aforementioned approaches.

The present paper presents a lattice-cell model, which allows one to overcome the restriction on Poisson's ratio while preserving the favorable properties of the classic lattice for simulating tensile fracture. The struts in the present model form triangular cells, which resist volume change and thereby introduce a coupling of the constitutive response of the struts. Poisson's ratio can be controlled by the ratios of the stiffnesses of the struts and the cells. The model is suitable for implementation in standard finite element programs, since the cells can be modeled by constant strain triangular elements and the trusses by ordinary truss elements. Tensile fracture is modeled by a reduction of the stiffness of the struts driven by the strain. The stiffness of the cells is kept proportional to the minimum stiffness of the surrounding trusses.

Firstly, the relationship of the material parameters of the lattice-cell model and the parameter's of Hooke's law of an elastic solid in plane strain are derived for the example of an equilateral triangle. The validity of these derivations is supported by numerical simulations of an elastic solid in uniaxial tension. Secondly, the elastic constitutive model of the trusses is extended to a damage model, which is used to simulate tensile fracture.

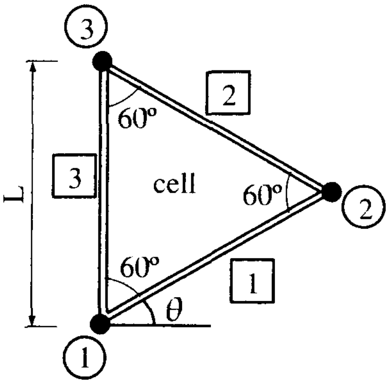

(a)

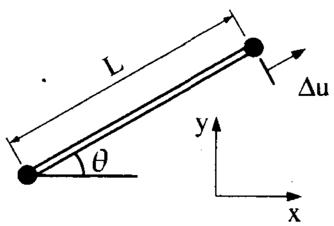

(b)

Figure 1. (a) Equilateral triangle composed of three struts and one cell. (b) A strut.

2 RELATIONSHIP TO ELASTIC CONTINUUM

In this section, the elastic response of a structure made of three trusses and one cell in the form of an equilateral triangle, shown in Figure 1a, is compared to the elastic continuum in plane strain. The force f in the strut is related to the normal stress σ as

$$f = \sigma A_t \tag{1}$$

where A_t is the cross-sectional area of the strut. The normal strain in the lattice strut is defined as

$$\varepsilon = \frac{\Delta u}{L} \tag{2}$$

where Δu is the relative displacement in the longitudinal direction and L is the length of the strut. Furthermore, an elastic stress-strain relation of the form

$$\sigma = E_t \varepsilon \tag{3}$$

is assumed, where E_t is the elastic modulus of the material of the strut. The energy stored in a single strut, shown in Figure 1b, is defined as

$$W_t = \frac{1}{2} f \Delta u = \frac{1}{2} E_t \varepsilon A_t L \tag{4}$$

Consequently, the energy of a triangle formed by three struts, shown in Figure 1a, results to

$$W = W_{t1} + W_{t2} + W_{t3} = \frac{1}{2} A_t L E_t \left(\varepsilon_1^2 + \varepsilon_2^2 + \varepsilon_3^2\right) \tag{5}$$

where the subscripts 1, 2, 3 refer to the respective struts. The energy in Equation 5 is transformed to strain energy by dividing it by the area of the cell A_c.

$$V_t = W/A_c = \frac{1}{6} E_t \left(\varepsilon_1^2 + \varepsilon_2^2 + \varepsilon_3^2\right) \tag{6}$$

where it is assumed that $A_t = A_c/(3L)$.

So far, the cell, which is formed by the struts, has not yet been considered. Since the cell resists volume change, an additional energy term is added and so the total energy results in

$$V = V_t + V_c = \frac{1}{6} E_t \left(\varepsilon_1^2 + \varepsilon_2^2 + \varepsilon_3^2\right) + \frac{1}{2} m E_t \varepsilon_V^2 \tag{7}$$

where ε_V is the volumetric strain in the cell, which is expressed in the form of normal components of the continuum strain as $\varepsilon_V = \varepsilon_{xx} + \varepsilon_{yy} + \varepsilon_{zz}$ (with $\varepsilon_{zz} = 0$ in plane strain). The parameter m is a model parameter, which relates the stiffness of the cell to the stiffness of the struts and is used to control the value of Poisson's ratio.

The normal strain in the direction of a strut, as shown in Figure 1b, is related to the Cartesian strain components as

$$\varepsilon(\theta) = \varepsilon_{xx} \cos^2(\theta) + \varepsilon_{yy} \sin^2(\theta) + \gamma_{xy} \cos(\theta) \sin(\theta) \tag{8}$$

where θ is the angle that the normal direction of the strut forms with the x-axis of the Cartesian coordinate system. Thus, the strain energy in Equation 7 can be expressed by the Cartesian strain components as

$$V = \frac{1}{16} E_t \left(3\varepsilon_{xx}^2 + 2\varepsilon_{xx}\varepsilon_{yy} + 3\varepsilon_{yy}^2 + \gamma_{xy}^2\right) + \frac{1}{2} E_t \left(\varepsilon_{xx}^2 + \varepsilon_{xx}\varepsilon_{yy} + \varepsilon_{yy}^2\right) \tag{9}$$

Here, γ_{xy} is the engineering shear strain, which is defined as $\gamma_{xy} = 2\varepsilon_{xy}$. The Cartesian stress components are defined as

$$\sigma_{xx} = \frac{\partial V}{\partial \varepsilon_{xx}} = E_t \left(\frac{3}{8} + m\right) \varepsilon_{xx} + E_t \left(\frac{1}{8} + m\right) \varepsilon_{yy} \tag{10}$$

$$\sigma_{yy} = \frac{\partial V}{\partial \varepsilon_{yy}} = E_t\left(\frac{1}{8}+m\right)\varepsilon_{xx} + E_t\left(\frac{3}{8}+m\right)\varepsilon_{yy} \tag{11}$$

and

$$\tau_{xy} = \frac{\partial V}{\partial \gamma_{xy}} = \frac{1}{8}E_t \tag{12}$$

where σ_{xx} and σ_{yy} are the normal stress components and $\tau_{xy} = \sigma_{xy}$ is the shear stress.

Hooke's law for the elastic continuum, on the other hand, defines the stresses by means of the Young's modulus E and Poisson's ratio ν as

$$\sigma_{xx} = \frac{E(1-\nu)}{(1+\nu)(1-2\nu)}\varepsilon_{xx} + \frac{E\nu}{(1+\nu)(1-2\nu)}\varepsilon_{yy} \tag{13}$$

$$\sigma_{yy} = \frac{E\nu}{(1+\nu)(1-2\nu)}\varepsilon_{xx} + \frac{E(1-\nu)}{(1+\nu)(1-2\nu)}\varepsilon_{yy} \tag{14}$$

and

$$\tau_{xy} = \frac{E}{2(1+\nu)}\gamma_{xy} \tag{15}$$

The relation of the parameters of the lattice-cell model (E_t, m) to the parameters of Hooke's law of the elastic continuum (E, ν) is determined by comparison of the coefficients of ε_{xx} and γ_{xy} in Equations 10 and 13, and 12 and 15, respectively. This leads to the equalities

$$\frac{E(1-\nu)}{(1+\nu)(1-2\nu)} = \frac{3}{8}E_t + mE_t \tag{16}$$

and

$$\frac{E}{2(1+\nu)} = \frac{1}{8}E_t \tag{17}$$

Thus, the expressions for ν and E result in

$$\nu = \frac{1+8m}{4+16m} \tag{18}$$

and

$$E = E_t\frac{5+24m}{16+64m} \tag{19}$$

Accordingly, m and E_t can be expressed by means of E and ν as follows:

$$m = \frac{4\nu-1}{8-16\nu} \tag{20}$$

and

$$E_t = \frac{4E}{1+\nu} \tag{21}$$

For the upper limit of Poisson's ratio ($\nu = 1/2$) the parameters of the lattice-cell model result in

$$\lim_{\nu\to\frac{1}{2}} m = \infty \tag{22}$$

and

$$\lim_{\nu\to\frac{1}{2}} E_t = \frac{8}{3}E \tag{23}$$

For the lower limit ($\nu = -1$), on the other hand, the parameters are found to be

$$\lim_{\nu\to-1} m = -\frac{5}{24} \tag{24}$$

and

$$\lim_{\nu\to-1} E_t = 0 \tag{25}$$

Furthermore, for the value $m = 0$, the classic lattice model with Poisson's ratio of $\nu = 1/4$ is regained. Consequently, Poisson's ratio less than 1/4 requires a negative m. The energy in Equation 7, however, must be guaranteed to be positive for all values of m. The condition for a positive strain energy can be determined by expressing the extra energy term associated with the volumetric strain of the cell by means of the strains in the adjacent struts; this gives

$$\varepsilon_V = \varepsilon_{xx} + \varepsilon_{yy} = \frac{2}{3}(\varepsilon_1+\varepsilon_2+\varepsilon_3) \tag{26}$$

Thus, the strain energy in Equation 7 can be written as

$$V = \frac{1}{6}E\left(\varepsilon_1^2+\varepsilon_2^2+\varepsilon_3^2\right) + \frac{2}{9}mE(\varepsilon_1+\varepsilon_2+\varepsilon_3)^2 \tag{27}$$

The strain energy is guaranteed to be positive if the eigenvalues of

$$[\nabla V] = \begin{pmatrix} \frac{\partial^2 V}{\partial \varepsilon_1^2} & \frac{\partial^2 V}{\partial \varepsilon_1 \partial \varepsilon_2} & \frac{\partial^2 V}{\partial \varepsilon_1 \partial \varepsilon_3} \\ \frac{\partial^2 V}{\partial \varepsilon_2 \partial \varepsilon_1} & \frac{\partial^2 V}{\partial \varepsilon_2^2} & \frac{\partial^2 V}{\partial \varepsilon_2 \partial \varepsilon_3} \\ \frac{\partial^2 V}{\partial \varepsilon_3 \partial \varepsilon_1} & \frac{\partial^2 V}{\partial \varepsilon_3 \partial \varepsilon_2} & \frac{\partial^2 V}{\partial \varepsilon_3^2} \end{pmatrix}. \tag{28}$$

are positive, which results in the condition

$$m > -\frac{1}{4} \tag{29}$$

This value is less than the lower limit of m in Equation 24. Thus, the strain energy is guaranteed to be positive for all possible values of Poisson's ratio.

As mentioned above, the resistance of the cell to volume change results in an additional energy term, which leads to a coupling of the struts, and so the stress in a strut depends not only on the strain in this strut, but also on the strains in the neighbors. The stress in strut 1, for instance, can be determined from Equation 27;

$$\sigma_1 = \frac{\partial V}{\partial \varepsilon_1} = \frac{1}{3}E_t\varepsilon_1 + \frac{4}{9}mE_t(\varepsilon_1 + \varepsilon_2 + \varepsilon_3) \tag{30}$$

3 NUMERICAL PREDICTION OF THE ELASTIC PROPERTIES

The theoretical derivations in the preceding Section are supported by numerical simulations of a solid in plane strain subjected to uniaxial tension. The geometry and boundary conditions of the specimen studied are shown in Figure 2a.

The dimensions of the specimen are set to $d = 0.1$ m and $h = 0.3$ m. The mesh, which was generated by means of the program T3D (Rypl (1998)), is shown in Figure 2b. Each triangle represents three trusses and one cell. The edge length of the triangles is approximately 7 mm.

The parameters E_t and m of the lattice model were varied to simulate different Poisson's ratios ν at a constant Young's modulus $E = 1$ using Equations 20 and 21. Poisson's ratio ν was determined by means of the average deformations in x- and y-directions, $\overline{\Delta u_x}$ and $\overline{\Delta u_y}$, at the boundary of the specimen as

$$\nu^{num} = \frac{\overline{\Delta u_x}h}{\overline{\Delta u_x}h - \overline{\Delta u_y}d} \tag{31}$$

A comparison of the theoretical and numerical Poisson's ratio is shown in Figure 3. It is seen that the agreement of theory and numerical simulation is good. The deviations for small Poisson's ratios ($\nu = -0.5$ and -0.99) might be due to the irregularity of the mesh used.

4 EXTENSION TO DAMAGE MECHANICS

To model fracture of concrete subjected to tensile loading, the elastic stress-strain relation of the struts was

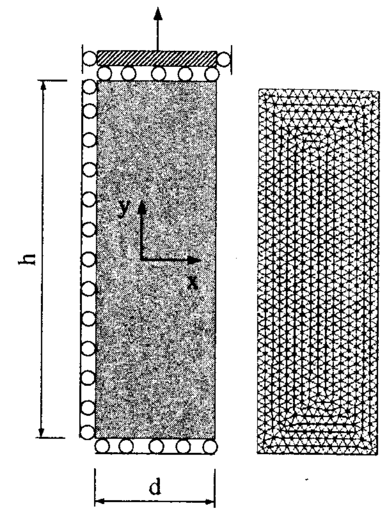

(a) (b)

Figure 2. (a) Geometry and loading setup. (b) Mesh.

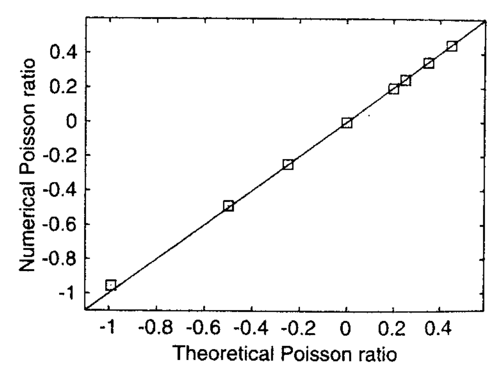

Figure 3. Comparison of the numerical and theoretical values of Poisson's ratio of the elastic solid in plane strain.

extended to an elasto-damage stress–strain relation of the form

$$\sigma = (1 - \omega)E_t\varepsilon \tag{32}$$

The damage variable ω is related to the history variable κ as

$$\omega = \begin{cases} 0 & \text{if } \kappa \leq \varepsilon_0 \\ 1 - \dfrac{\varepsilon_0}{\kappa}\exp\left(-\dfrac{\kappa - \varepsilon_0}{\varepsilon_f}\right) & \text{if } \kappa \geq \varepsilon_0 \end{cases} \tag{33}$$

where $\varepsilon_0 = f_t/E_t$ is the strain at peak stress and ε_f is a parameter that controls the initial slope of the exponential softening curve. The parameter f_t is the tensile strength of the strut. The history variable κ is defined by the loading function

$$f(\varepsilon, \kappa) = \langle\varepsilon\rangle - \kappa \tag{34}$$

along with the loading and unloading conditions

$$f(\varepsilon,\kappa)\leq 0,\quad \dot{\kappa}\geq 0,\quad \dot{\kappa}f(\varepsilon,\kappa)=0 \tag{35}$$

The symbol $\langle\ldots\rangle$ in Equation 34 is the positive-part operator, defined as $\langle x\rangle = \max(x,0)$.

To ensure that the total energy stored in the material remains positive during damage evolution, the secant stiffness of the cell is determined by means of the maximum damage variable of the adjacent struts. Thus, the energy of the equilateral triangle (Figure 1a) for the damaged state results in

$$V = \frac{1}{6}E_t\left((1-\omega_1)\varepsilon_1^2 + (1-\omega_2)\varepsilon_2^2 + (1-\omega_3)\varepsilon_3^2\right) + \frac{1}{2}mE_t(1-\omega_{max})\varepsilon_V^2 \tag{36}$$

where $\omega_1, \omega_2, \omega_3$ are the damage variables of the three trusses and ω_{max} is the maximum of those values.

5 PLAIN CONCRETE SUBJECTED TO DIRECT TENSION

The model is applied to the simulation of plain concrete subjected to quasi-static tensile loading in plane strain conditions. The geometry and the loading setup are shown in Figure 4. The rotation and the lateral expansion of the ends of the specimen are not restrained. The dimensions are chosen again to be $h=0.3$ m and $d=0.1$ m. It is known that the fracture patterns obtained with lattice (or particle) models are often strongly influenced by the structure of the mesh (Jirásek and Bažant (1995b)). Therefore, the vertices of the mesh for the fracture simulation are placed randomly, as shown in Figure 5a.

To avoid too small elements, a minimum distance of the vertices of $d_{min}=5$ mm was enforced. Additionally, vertices were placed at the boundary of the specimen with a regular spacing of d_{min}. The mesh generation (see Figure 5b) was based on a Delaunay triangulation using the program Triangle (Shewchuk (1996)).

The elastic material parameters of the lattice-cell model are chosen to $E_t=66.67$ GPa and $m=-0.04167$, which corresponds, according to Equations 18 and 19, to $E=20$ GPa and $\nu=0.2$. Furthermore, the parameter that controls the slope of the softening curve is chosen as $\varepsilon_f=0.01$. Finally, the parameter ε_0 was chosen to be randomly distributed according to the Weibull cumulative distribution function

$$P_w = 1-\exp\left[-\left(\frac{\varepsilon_0}{s_1}\right)^k\right] \tag{37}$$

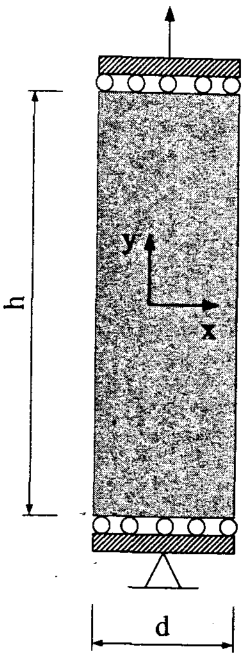

Figure 4. Geometry and loading setup.

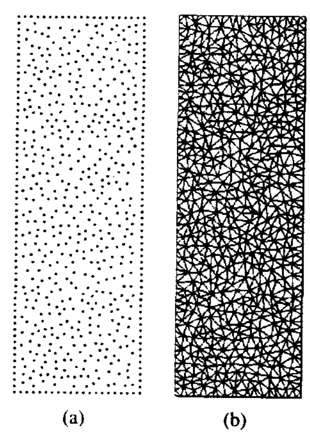

Figure 5. (a) Random distribution of vertices. (b) Mesh.

where the Weibull modulus is set as $k=6$ and the scaling factor to $s_1=0.00018$, which corresponds to a peak stress of the stress-strain relation of the strut of $f_t=E_t\varepsilon_0=12$ MPa.

The load-displacement curve is shown in Figure 6. Furthermore, the damage pattern is presented in Figure 7 for three stages (marked in Figure 6). The struts, in which the damage variable increases, are marked by black lines and those in which the nonzero damage variable remains constant by gray lines.

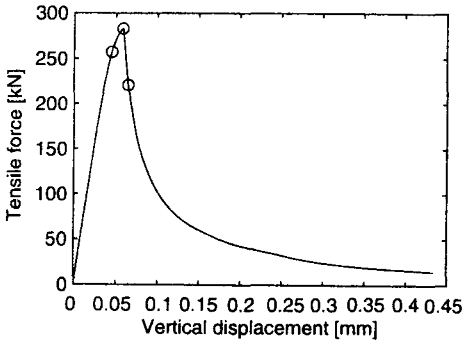

Figure 6. Load-displacement curve of the concrete specimen in plane strain subjected to tension.

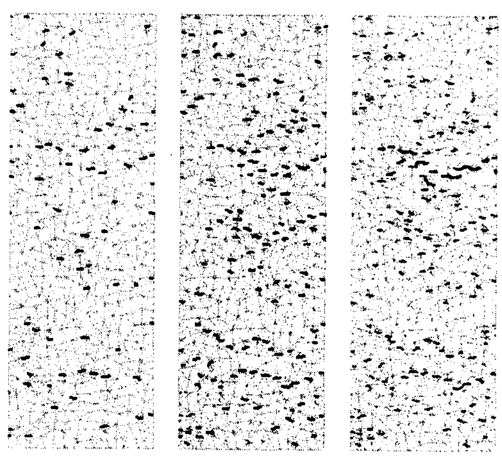

Figure 7. Damage in the trusses for three stages of analysis (marked in Figure 6). Lattice struts with increasing damage variable are marked by black lines and those with a constant nonzero damage variable by gray lines.

The simulation gives a realistic description of the response of concrete under tensile loading with regard to both the load-displacement curve and the crack patterns obtained.

6 CONCLUSIONS

A lattice cell model, in which the lattice struts form triangular cells resisting volume change is explored. The model is capable of predicting the full range of Poisson's ratio of an elastic solid in plane strain, as demonstrated both analytically and numerically. Furthermore, the model yields the typical behavior of quasibrittle materials under tensile loading. It is intended to extend this modeling approach to three dimensions and to apply it to Monte Carlo simulations of concrete structures.

ACKNOWLEDGMENTS

The work was supported under U.S. National Science Foundation grant CMS-0301145 to Northwestern University. The simulations were performed using the object-oriented finite element package OOFEM (Patzák (1999), Patzák and Bittnar (2001)) extended by the present writers.

REFERENCES

Bažant, Z.P., M.R. Tabbara, M. T. Kazemi, and G. Pijaudier-Cabot (1990). Random particle model for fracture of aggregate or fiber composites. *Journal of Engineering Mechanics, ASCE 116*, 1686–1705.

Cusatis, G., Z.P. Bažant, and L. Cedolin (2003a). Confinement-shear lattice model for concrete damage in tension and compression: I. Theory. *Journal of Engineering Mechanics, ASCE 129*, 1439–1448.

Cusatis, G., Z.P. Bažant, and L. Cedolin (2003b). Confinement-shear lattice model for concrete damage in tension and compression: II. Computation and validation. *Journal of Engineering Mechanics, ASCE 129*, 1449–1458.

Griffiths, D. V. and G. G.W. Mustoe (2001). Modelling of elastic continua using a grillage of structural elements based on discrete element concepts. *International Journal for Numerical Methods in Engineering 50*, 1759–1775.

Jirásek, M. and Z.P. Bažant (1995a). Macroscopic fracture characteristics of random particle systems. *International Journal of Fracture 69*, 201–228.

Jirásek, M. and Z.P. Bažant (1995b). Particle model for quasibrittle fracture and application to sea ice. *Journal of Engineering Mechanics, ASCE 121*, 1016–1025.

Morikawa, O., Y. Sawamota, and N. Kobayashi (1993). Local fracture analysis of a reinforced concrete slab by the discrete element method. In M. Press (Ed.), *Proceedings of the 2nd International Conf. on Discrete element methods*, pp. 275–286. held in Cambridge, MA, USA.

Patzák, B. (1999). Object oriented finite element modeling. *Acta Polytechnica 39*, 99–113.

Patzák, B. and Z. Bittnar (2001). Design of object oriented finite element code. *Advances in Engineering Software 32*, 759–767.

Rypl, D. (1998). *Sequential and Parallel Generation of Unstructured 3D Meshes*. Ph. D. thesis, Czech Technical University, Prague, Czech Republic.

Schlangen, E. and J. G. M. van Mier (1992). Simple lattice model for numerical simulation of fracture of concrete materials and structures. *Materials and Structures 25*, 534–542.

Shewchuk, J. R. (1996, May). Triangle: Engineering a 2D Quality Mesh Generator and Delaunay Triangulator. In M. C. Lin and D. Manocha (Eds.), *Applied Computational Geometry: Towards Geometric Engineering*, Volume 1148 of *Lecture Notes in Computer Science*, pp. 203–222. Springer-Verlag. From the First ACM Workshop on Applied Computational Geometry.

Zubelewicz, A. and Z.P. Bažant (1987). Interface modeling of fracture in aggregate composites. *Journal of Engineering Mechanics, ASCE 113*, 1619–1630.